Investigation of the role of cell hydrophobicity and EPS production in the aggregation of the marine diatom Cylindrotheca closterium under hypo-saline conditions

Irem Demir-Yilmaz, Nives Novosel, Maja Levak Zorinc, Tea Mišić Radić, Malak Souad Ftouhi, Pascal Guiraud, Nadica Ivošević Denardis, Cécile Formosa-Dague

Investigation of the role of cell hydrophobicity and EPS production in the aggregation of the marine diatom *Cylindrotheca closterium* under hypo-saline conditions

Irem Demir-Yilmaz[1,2,‡], Nives Novosel[3,‡], Maja Levak Zorinc[3], Tea Mišić Radić[3], Malak Souad Ftouhi[1], Pascal Guiraud[1,4], Nadica Ivošević DeNardis[3*] and Cécile Formosa-Dague[1,4*]

[1] TBI, Université de Toulouse, INSA, INRAE, CNRS, Toulouse, France

[2] LAAS, Université de Toulouse, CNRS, Toulouse, France

[3] Division for Marine and Environmental Research, Ruđer Bošković Institute, Zagreb, Croatia

[4] Fédération de Recherche Fermat, CNRS, Toulouse, France

‡ These two authors equally contributed to the work

Corresponding authors:

Cécile Formosa-Dague, formosa@insa-toulouse.fr, Nadica Ivošević DeNardis, ivosevic@irb.hr

Abstract

Aggregation of diatoms is of global importance to understand settling of particulate organic carbon in aquatic systems. In this study, we investigate the aggregation of the marine diatom *Cylindrotheca closterium* during the exponential growth phase under hypo-saline conditions. The results of the flocculation/flotation experiments show that the aggregation of the diatom depends on the salinity. In favorable growth conditions for marine diatoms (salinity of 35), the highest aggregation is achieved. To explain these observations, we used a surface approach combining atomic force microscopy (AFM) and electrochemical methods to characterize both the cell surface properties and the structure of the extracellular polymeric substances (EPS) cell produce, and to quantify the amount of surface-active organic matter released. At a salinity of 35, the results showed that diatoms are soft, hydrophobic and release only small amounts of EPS organized into individual short fibrils. In contrast, diatoms adapt to a salinity of 5 by becoming much stiffer and more hydrophilic, producing larger amounts of EPS that structurally form an EPS network. Both adaptation responses of diatoms, the hydrophobic properties of diatoms and the release of EPS, appear to play an important role in diatom aggregation and explain the behavior observed at different salinities. This biophysical study provides important evidence allowing to get a deep insight into diatom interactions at the nanoscale, which may contribute to a better understanding of large-scale aggregation phenomena in aquatic systems.

Keywords: aggregation, atomic force microscopy, cell hydrophobicity, *Cylindrotheca closterium*, extracellular polymeric substances, hypo-saline stress

1. INTRODUCTION

Diatoms form a very diverse group of eukaryotic microalgae (100,000 species) found in all aquatic environments (fresh and marine waters, soils and terrestrial systems), either in benthic or planktonic states. They are thought to be responsible for 20% of the total production on Earth and 40% of the total marine primary production (Scala and Bowler, 2001). In particular, *Cylindrotheca closterium* is a widespread marine diatom in coastal and estuarine environments that can develop in both planktonic and benthic states. On the mudflats found in these regions, this species forms biofilms on the surface of sediments, increasing their stability and promoting the deposition of sediment particles (de Brouwer et al., 2005). When these biofilms are then disturbed, cells become resuspended in the water and continue to live in the planktonic state (Thornton, 2002). In both the benthic and planktonic states, this species can produce large amounts of extracellular polymeric substances (EPS), which it requires for locomotion or to promote its adhesion to the substrate and subsequent biofilm formation (Staats et al., 2000). In the planktonic state, these EPS can be involved in the aggregation (*i.e.*, flocculation) of cells that can then form marine snow, *i.e.*, aggregates of detritus, inorganic material, and living organisms greater than 0.5 mm in diameter (Iversen and Ploug, 2013). Macroaggregates can even reach meter or kilometer scales, as demonstrated by the phenomenon of macroscopic gel formation in the northern Adriatic Sea, which has been shown to be related to the production of extracellular polymers by the dominant diatom species *C. closterium* (Alcoverro et al., 2000; Kovač et al., 2005; Najdek et al., 2005; Pletikapić et al., 2011; Radić et al., 2011; Svetličić et al., 2011; Žutić and Svetličić, 2000). Moreover, these aggregates then sediment and export organic matter such as carbon from the surface to the deep sea, a phenomenon referred to as the biological carbon pump (Piontek et al., 2009; Tréguer et al., 2018).

In coastal and estuarine environments where diatoms such as *C. closterium* occur, salinity is usually a local environmental factor that can vary widely (Glaser and Karsten, 2020). In open oceans, salinity is relatively constant due to intense mixing, but in nearshore or estuarine waters where riverine freshwater mixes with marine water, the degree of salinity dilution is highly variable (Karsten, 2012). In addition, future climate change scenarios foresee less precipitation and more evaporation in these zones, which will lead to further changes in salinity (Glaser and Karsten, 2020). For these reasons, the effects of salinity changes (hypo- or hyper-saline) on diatoms such as *C. closterium* have been the subject of several studies. For example, authors have shown that changes in salinity can have effects on cell motility (Apoya-Horton et al., 2006; Araújo et al., 2013), cell length (De Miranda et al., 2005), cell growth (Araújo et al., 2013; Glaser and Karsten, 2020; Rijstenbil, 2005; Van Bergeijk et al., 2003), EPS production (Najdek et al., 2005; Steele et al., 2014) or oxidative stress (Roncarati et al., 2008). Studies using other estuarine diatom species such as *Thalassiosira weissflogii* have also showed that salinity changes could also influence the transcriptomic activities of cells (Bussard et al., 2017). In the specific case of *C. closterium*, a recent study from our group investigated the effects of salinity changes on the surface properties and EPS production of *C. closterium* cells in the stationary phase, which determines their functional behavior in aquatic systems (Novosel et al., 2022a). For that, cell adhesive and nanomechanical properties were probed using atomic force microscopy (AFM), which is a powerful technique to study microalgae at the nanoscale and probe their biophysical properties (Demir-Yilmaz et al., 2021). Moreover, AFM has also been used before to elucidate the molecular mechanisms underlying microalgae cell aggregation for different types of microalgae species showing, its interest in such studies (Besson et al., 2019; Demir et al., 2020; Demir-Yilmaz et al., 2022; Formosa-Dague et al., 2018; Vergnes et al., 2019).

To date, no studies have examined the effects of salinity on diatom aggregation during the exponential growth phase. Thus in this work, we investigate how hypo-saline conditions (15 and 5) affect the aggregation of *C. closterium* in this growth phase using flocculation/flotation experiments. In addition, AFM was used to determine nanomechanical and hydrophobic properties of diatoms and the structural organization of EPS, while an electrochemical approach allowed quantification of released surface-active organic matter. Overall, this original data set contributes to the understanding of the mechanism underlying cell aggregation of *C. closterium* under hypo-saline conditions. Such data are important for understanding globally important processes that occur in marine waters, such as the formation of marine snow.

2. MATERIAL AND METHODS

2.1. Microalgae strain and culture conditions

The diatom *Cylindrotheca closterium* (Bacillariophyceae, CCMP 1554, Culture Collection Bigelow Laboratory for Ocean Sciences, Bigelow, MN, USA) was cultured under sterile conditions in natural seawater (salinity of 35) and enriched with f/2 medium (Guillard, 1975). Diatom monocultures were grown in both laboratories (at the Ruder Boskovic Institute (RBI) and at Toulouse Biotechnology Institute (TBI)) using seawater from the southern Adriatic Sea and the Mediterranean Sea. In both cases, the culture medium was sterilized before use by autoclave. Cells were cultured either in flasks (50 to 100 mL) at 19°C and 120 rpm in an incubator with white neon tubes providing an illumination of 40 µmol photons m^{-2} s^{-1} with a photoperiod of 18 hours light:6 hours dark, or in a water bath at 19°C and 20 rpm and a photoperiod of 12 hours light:12 hours light with an irradiance of 32 µmol photons m^{-2} s^{-1}. Both types of cultivation resulted in similar growth rates under the different conditions tested in this study. To induce salinity stress, natural seawater was diluted with sterile MilliQ water to obtain selected salinities of 15 and 5, and cells were cultured under the same conditions for 7 days. To monitor cell growth, the average cell abundance in duplicate samples was determined using a Fuchs-Rosenthal hemocytometer (Fein-Optik Jena, Germany, depth 0.2 mm) and a light microscope (Olympus BX51, Olympus Corporation, Japan). Growth rate and doubling time were determined in the early exponential growth phase of diatoms (Kim, 2015).

2.2. Electrochemical method

The electrochemical method of polarography at the dropping mercury electrode allows characterization of released surface-active organic matter from cell culture (Pletikapić and Ivošević DeNardis, 2017; Svetličić et al., 2006). Here, adsorption of organic matter and submicron particles on the dropping mercury electrode leads to a decrease in the surface tension gradient at the mercury interface, which causes the suppression of convective flow proportional to the surfactant concentration in the sample and is referred to as surfactant activity. The surfactant activity of seawater can be expressed as the equivalent amount of the nonionic synthetic surfactant used, Triton-X-100 (polyethylene glycol tert-octylphenyl ether), in milligrams per liter.

2.3. Electrochemical measurements

Electrochemical measurements were performed in an air-permeable and thermostatic Metrohm vessel with a three-electrode system. The dropping mercury electrode served as the working electrode and had the following characteristics: dropping time: 2.0 s, flow rate: 6.0 mg s^{-1}, maximum surface area: 4.57 mm^2. All potentials were referenced to a potential measured at a reference electrode, i.e., Ag/AgCl (0.1 M NaCl) separated from the measured dispersion by a ceramic frit. A platinum wire was used as a counter electrode. Electrochemical measurements were performed using a 174A Polarographic Analyzer (Princeton Applied Research, Oak Ridge, TN, USA) connected to a computer. Analogue data acquisition was performed using a DAQ card-AI-16-XE-50 (National Instruments, Austin, TX, USA). Data analysis was performed using the application developed in LabView 6.1 software (National Instruments, Austin, TX, USA). Electrochemical measurements of the surfactant activity of the sample were performed by recording polarograms of Hg(II) reduction (current-potential curves) at a scan rate of 10 mV/s. The nonionic surfactant Triton-X-100 (polyethylene glycol tert-octylphenyl ether, Sigma) was used as a standard. Stock solutions of Triton-X-100 (10 g/L) were prepared in artificial seawater with the corresponding salinities. The polarographic maximum Hg(II) was measured for a range of Triton-X-100 concentrations, and

surfactant activities were determined at -350 mV, which was used to construct calibration curves. Surfactant activity of *C. closterium* cell cultures in the exponential growth phase was measured by adding 0.5 mL of 0.1 M $HgCl_2$ to the sample and recording the polarographic maximum of Hg(II).

2.4. AFM imaging of living cell

Before AFM imaging experiments, cells were harvested by centrifugation (2000 *g*, 3 min) and washed twice in Phosphate Buffer Saline (PBS) buffer at pH 7.4. AFM images of *C. closterium* cells were acquired with cells immobilized on positively charged glass slides (SuperfrostTM Plus Adhesion, Epredia, USA) in PBS at pH 7.4. The quantitative imaging mode of Nanowizard III AFM (Bruker, USA) with MSCT cantilevers (Bruker, nominal spring constant of 0.01 N/m) was used. Images were acquired at a resolution of 80 pixels, with an applied force of < 1.5 nN and a constant approach/retract speed ranging from 180 to 200 µm/s (z-range of 1.5 µm). For roughness measurements, images were acquired on areas of 0.5 × 0.5 µm in contact mode with MSCT cantilevers at an applied force < 0.5 nN. In all cases, the spring constants of the cantilevers were determined using the thermal noise method prior to imaging (Hutter and Bechhoefer, 1993).

2.5. AFM imaging of EPS

Atomic force microscopy images of EPS were acquired using a Multimode Scanning Probe Microscope with Nanoscope IIIa controller (Bruker, Billerica, MA, USA) equipped with a 125 µm vertical engagement (JV) scanner. *C. closterium* diatoms cultured at salinities of 5, 15, and 35 were separated from the growth medium by gentle centrifugation (2000 *g*, 3 min) on day 7 of growth. The loose pellet was washed twice with filtered seawater of the corresponding salinity, diluted to a final volume of 1 mL with filtered seawater, and used to prepare samples for AFM measurements. A 5 µL aliquot of the cell suspension was pipetted onto freshly cleaved mica and placed in a closed Petri dish for 1 hour to allow the cells to settle and attach to the surface. The mica discs were then immersed in ultrapure water three times for 30 seconds and dried. After the drying step, the discs were taped to a metal sample pack with double-sided tape and imaged with the AFM. Imaging was performed in contact mode in air with silicon nitride cantilevers (DNP, Bruker, nominal frequency 18 kHz, nominal spring constant 0.06 N m^{-1}). The linear scan rate was between 1.5 and 2 Hz and the scan resolution was 512 samples per line. To minimize the interaction forces between the tip and the surface, the set point was kept at the lowest possible value. Image processing and analysis was performed using NanoScopeTM software (Bruker, Billerica, MA, USA).

2.6. Force spectroscopy measurements

For nanoindentation measurements, cells were harvested by centrifugation (2000 *g*, 3 min), washed twice in PBS buffer at pH 7.4, and immobilized on positively charged glass slides (SuperfrostTM Plus Adhesion, Epredia, USA). In these experiments, a cantilever with known mechanical properties is pressed against the cell surface with a specific force. In this way, the Ym value of the cell can be determined, a value that reflects its resistance to compression and thus its rigidity. In this study, nanoindentation measurements were performed on 10 cells from 2 independent cultures under all conditions, and 400 force curves were recorded for each cell on areas of 500 × 500 nm on the cell surface. Force spectroscopy experiments were performed with an applied force between 1 and 3 nN depending on the condition using MLCT AUWH cantilevers with nominal spring constants of 0.1 N/m. Young's moduli were calculated from 40 nm indentation curves using the Hertz model (Hertz, 1881) in which the force F, indentation (δ), and Young's modulus (Ym) follow equation (1):

$$F = \frac{2 \times Ym \times tan\alpha}{\pi \times (1 - \upsilon^2) \times \delta^2} \quad (1)$$

Here α is the opening angle of the tip (17.5°) and υ is the Poisson's ratio (which is arbitrarily assumed to be 0.5). The spring constants of the cantilevers were determined before each experiment using the thermal noise method (Hutter and Bechhoefer, 1993).

2.7. Hydrophobicity measurements

To measure the hydrophobic properties of cells, a recently developed method was used, which consists of using fluidic force microscopy (FluidFM) to measure the interactions between a bubble (hydrophobic surface) and cell surfaces (Demir et al., 2021). For this purpose, FluidFM probes with an aperture of 8 µm in diameter (Cytosurge AG, Switzerland) were hydrophobized by coating with self-assembled monolayers (SAMs) of silanes using SAMs vapor deposition technique. The FluidFM cantilevers were functionalized with 1H,1H,2H,2H-perfluorodecyltrichlorosilane (FDTS) using an Orbis-1000 equipment (Memsstar, Livingston, UK) to make their outer surface and the inner surface of the microchannel hydrophobic. The deposition was carried out under vacuum at 40 Torr and -40°C for 5 minutes. Then, the microchannel of these silanized cantilevers was filled with air and the probe was immersed in PBS 1X. A slight overpressure of 20 mbar was applied to remove any particulate or dust contamination or to prevent clogging of the FluidFM cantilever. To create a bubble at the opening of the cantilever, a positive pressure of 200 mbar was then applied inside the microfluidic cantilever in buffer. The silanized probes were calibrated using the thermal noise method before each measurement (Hutter and Bechhoefer, 1993). The interactions between the generated bubbles and *C. closterium* cells under the selected salinities were then recorded in force spectroscopy mode, applying a maximum force of 1 nN and a constant retraction speed of 2 µm/s. For each condition, areas of 0.5 × 0.5 µm were examined on 5 different cells coming from two independent cultures. Adhesion forces were determined by calculating the maximum adhesion force from the obtained retraction force curves.

2.8. Flocculation/flotation separation experiments

Flocculation/flotation separation of *C. closterium* was performed in dissolved air flotation (DAF) experiments in a homemade flotation system as described elsewhere (Besson and Guiraud, 2013; Demir-Yilmaz et al., 2022, p.). For this purpose, algal suspensions with an optical density (750 nm) of 0.6 at salinities of 35 and 15 and with an optical density (750 nm) of 0.3 at salinity of 5 were used directly after 7 days of culture. For some experiments, cells were washed (2000 g, 3 min) and resuspended in PBS to remove EPS present in the culture medium. In these cases, the separation experiments were performed in PBS at a pH equal to that of the cells at the end of the cultures (9.4), eliminating the possible effects of pH fluctuations on cell flocculation. The cell suspensions were then added to the flocculation/flotation jars, and shaken (100 rpm) for 15 min to initiate flocculation. Depressurization at atmospheric pressure of deionized water saturated with air at 6 bar resulted in the formation of bubbles. Algae-free water was pressurized for 30 minutes before injection into the jars. Injection was controlled by a solenoid valve and 20 mL of pressurized water was added to each beaker sample. For all conditions, the algal suspension was removed from the bottom of the test-jars after 15 minutes: The first 5 mL of the treated phase was discarded, and the next 20 mL was used to quantify the flocculation/flotation efficiency. For this purpose, the optical density of the extracted microalgal suspension was measured and compared to the optical density of the microalgal suspension measured before the experiments. The flotation efficiency (E) was calculated according to the following equation 2:

$$E = \frac{OD_i.V_i - OD_f.V_f}{OD_i.V_i} \quad (2)$$

Where OD_i and OD_f are the initial and final optical densities (750 nm), respectively, and V_i and V_f are the initial and final volumes after addition of the bubbles.

2.9. Statistical analysis

Experimental results represent the mean ± standard deviation (SD) of at least three replicates. For each experiment, the number of replicates is indicated in the caption of the figures. For large samples (> 20), student t-test was used to assess the difference observed in the results. For small samples (between 10 and 20), when relevant, Mann and Whitney test was used to assess the difference. The differences were considered significantly at $p < 0.05$.

3. RESULTS

3.1. Salinity change affects growth dynamics of *C. closterium* cells

The growth curves obtained for *C. closterium* at the three selected salinities 5, 15, and 35 are shown in Figure 1. The initial abundance of cells in the growth medium was approximately 4.0×10^4 cells/ml. The highest cell number on the day 7 of growth was recorded in cultures with salinity 35, while the cell number was 7 times lower with salinity 5. Diatom growth is salinity dependent, such that the fastest growth rate of 0.40 day^{-1} and the shortest doubling time of 1.71 days were obtained at a salinity of 35, while the growth rate of 0.11 day^{-1} and the longest doubling time of 6.11 days were obtained at a salinity of 5. The same cell species was grown independently in another laboratory and also characterized at day 7 of growth. Figure S1 shows the corresponding growth curves of *C. closterium* at the selected salinities. Despite the different culture conditions in terms of illumination and photoperiod, the cell growth dynamics are similar in both cases and thus the data can be compared.

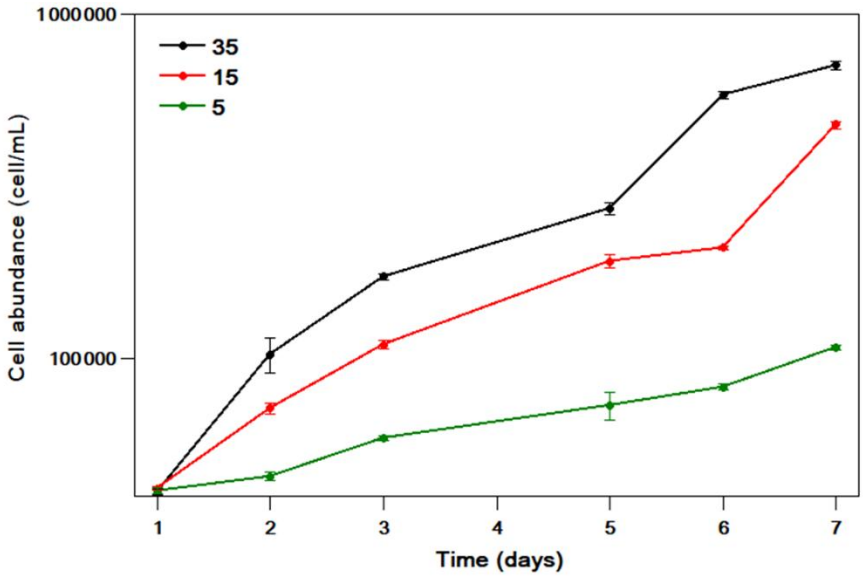

Figure 1. Growth curves of C. closterium at the selected salinities (5, 15 and 35). *Cells were cultivated in marine water enriched with f/2 medium in a water bath at 20 rpm and a photoperiod of 12 hours light:12 hours light with an irradiance of 32 µmol photons m^{-2} s^{-1}. The y-scale is logarithmic. Three different cultures in each salinity conditions were monitored.*

3.2. Salinity change affects the aggregation behavior of *C. closterium* cells

To evaluate the effects of salinity change on the aggregation of cells, flocculation/flotation experiments were performed. In this type of experiments, after 7 days of culture, the cell suspension is introduced in a flotation jar and mixed during 20 minutes to allow the cells to aggregate. Then, small bubbles generated by dissolved air flotation (DAF) are introduced at the bottom of the suspension; as they rise, they capture the aggregates formed and bring them to the surface. This separation is only possible if the cells are already aggregated. Thus, the separation efficiency obtained directly reflects the aggregation of the cells. These experiments were performed with cells directly after culture or with cells previously washed by centrifugation in buffer. The centrifugation process probably mainly removes EPS from the cells, as shown in Figure S2. Since EPS are a known factor promoting cell aggregation (Vergnes et al., 2019), including in the case of diatoms (Steele et

al., 2014), it is important to evaluate their potential involvement in cell aggregate formation. The results are shown in the histogram in Figure 2; the dark bars show the separation efficiency without washing the cells and the light bars with a washing step. When the cell cultures are used directly for the flocculation experiments (dark bars in Figure 3), the measured separation efficiency for cells cultured at a salinity of 35 is 64.6 ± 9.4%, which is quite high considering that no external flocculants were used. When the salinity is decreased, this efficiency drops to 53.7 ± 5.0% at a salinity of 15 and even further to 37.4 ± 6.0% at a salinity of 5. Statistical analysis showed that these differences between salinities 35 and 5 and between salinities 5 and 15 were significant (p-value of 0.01, Mann and Whitney test). When the experiments are repeated with cells separated and washed from the growth medium prior to the flocculation experiments and from which the EPS were mainly removed, we can see that all separation efficiencies decrease by the same factor of approximately 3. Under these conditions, the separation efficiency is 21.7 ± 13.5% at a salinity of 35 and decreases to 19.0 ± 9.9% at a salinity of 15 and to 11.5 ± 3.1% at a salinity of 5. Thus, the removal of EPS from cells has a significant effect on their aggregation behavior, but nevertheless, cells at a salinity of 35 are able to

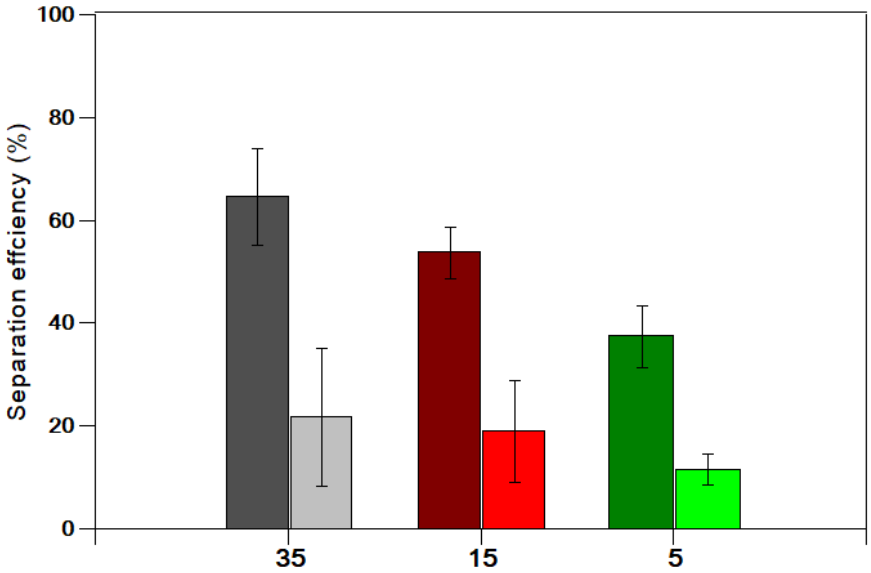

form more aggregates than cells at lower salinities. Hypo-salinity thus has a negative effect on cell aggregation.

Figure 2. Flocculation/flotation of C. closterium cells cultures at selected salinities. *The histogram shows the separation efficiency of C. closterium cells grown at salinities of 35, 15, and 5. The dark bars were obtained with direct cell cultures and the light bars with cells previously washed in phosphate buffer. In each case, the tests were repeated at least 7 times with three independent cultures.*

3.3. Salinity change affects the surface properties of cells

To understand the decrease in the ability of cells to aggregate under hypo-saline conditions, we examine the effects of selected salinities on cell surface roughness, nanomechanical properties, and hydrophobicity. Figure 3a-c show AFM height images of *C. closterium* cells at salinities studied. From these images, the reduction in salinity does not seem to affect the morphology of the cells, as they have similar shapes and dimensions. Then, to evaluate whether the salinity conditions tested in our study could have an effect on the nanostructure of the cell wall, we performed roughness measurements. For this purpose, high-resolution images of small areas (500 × 500 nm) were acquired

and used to measure the average roughness Ra. Under each condition, the measurements were performed on 10 cells from 2 independent cultures (Table S1). Figure 3d shows the distribution of these values. First, we note that the cell wall of *C. closterium* is quite smooth; at salinity of 35 (control), the roughness averages 0.8 ± 0.2 nm. As salinity decreases, the roughness of *C. closterium* cells also appears to decrease. However, statistical analysis (Mann and Whitney test) showed that the observed differences were not significant at a p-value < 0.05. Another important property of the cell surface that may change as a function of conditions is the rigidity of the cell wall. To obtain quantitative information about these properties, the elastic modulus (Ym) of the cell wall was determined by analyzing the force curves obtained during the nanoindentation measurements. The distribution of Ym values obtained (n = 4000 under each condition) is shown in Figure 3e (Table S2). Cells grown at a salinity of 35 have an average Ym value of 2.7 ± 1.1 MPa. *C. closterium* contains silica in its cell wall, which explains the high rigidity obtained here. As salinity decreases, the Ym value increases to 3.0 ± 0.7 MPa at a salinity of 15 and to 3.9 ± 1.9 MPa at a salinity of 5. Statistical analysis showed that the differences in this case were significant (two-sample t-test). Thus, when cells are subjected to hypo-saline conditions, cell rigidity increases, probably due to molecular changes in the cell wall under these conditions.

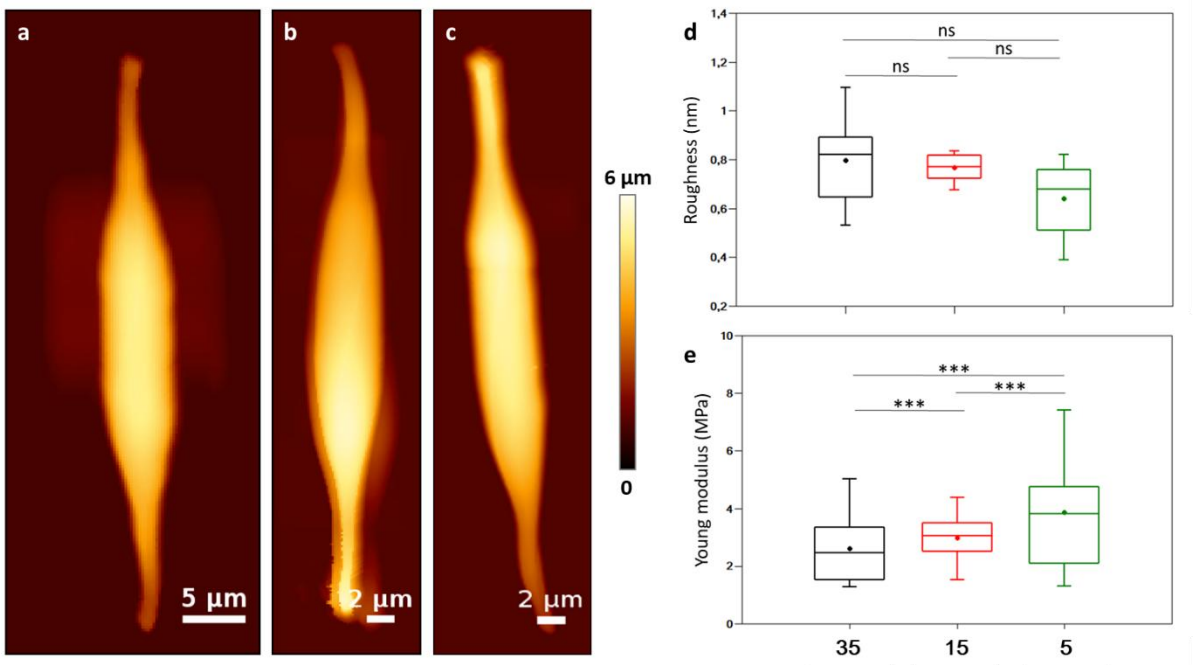

Figure 3. Nanostructural and nanomechanical characterizations of C. closterium cells at selected salinities. *AFM height images of single C. closterium cells cultured for 7 days in medium with salinity of (a) 35, (b) 15, and (c) 5. (d) Box plot showing the distribution of roughness values, each measured on 10 different cells from 2 independent cultures (Table S1). (e) Box plot showing the distribution of Ym values that reflects the cell surface rigidity, each measured on 10 different cells from two independent cultures (Table S2).*

We therefore investigated hydrophobic properties, using a recently developed technique in our team that consists in probing the interactions between cells and air bubbles produced using FluidFM technology (Demir et al., 2021), which combines AFM with microfluidics (Meister et al., 2009). This technique provides an accurate way to study the hydrophobic properties of complex

surfaces such as microalgal cells, where measuring water contact angle (WCA) can be difficult. Since air bubbles in water behave like hydrophobic surfaces, the stronger the interaction with the bubbles, the more hydrophobic the surface. The results of these experiments are shown in Figure 4. In each case, 5 cells from 2 independent cultures were examined (Table S3). They show that cells grown at a salinity of 35 interact with bubbles with an adhesion force of 367.6 ± 87.0 pN (Figure 4a). The adhesion force decreases for cells grown at a salinity of 15 (Figure 4b), with an average value of 108.5 ± 69.8 pN. At a salinity of 5, the cells no longer interact with the bubbles (no interactions recorded, Figure 3c). Therefore, the reduction in salinity affects the hydrophobic properties of the cells, as the cells become more hydrophilic under hypo-saline conditions.

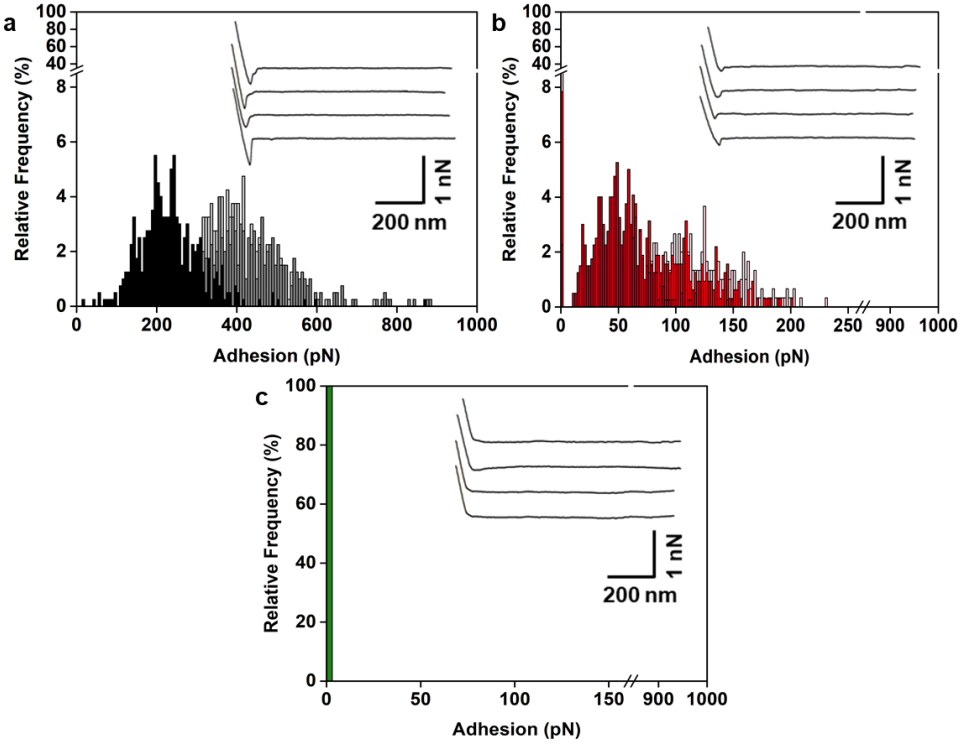

Figure 4. Probing the interactions between air bubbles and C. closterium cells cultured at the selected salinities. *Adhesion force histogram obtained for the interaction of air bubbles with C. closterium cells cultured at salinities of (a) 35, (b) 15 and (c) 5. The insets in the histograms show the representative force curves obtained during the force spectroscopy experiments. In each case, five cells coming from two independent cultures were used for measurements.*

3.4. Salinity change affects the production and nanostructural organization of released EPS

We determined the amount of released surface-active organic matter at the selected salinities, and characterized its nanostructural organization using the electrochemical method of polarography at the dropping mercury electrode and AFM, respectively. For this purpose, diatom cultures grown at the selected salinities were characterized in terms of surfactant activity per cell, which reflects the physiological activity of the cells. The results show that the surfactant activity is highest for the *C. closterium* culture grown at a salinity of 5 (13.9 pg T-X-100/L), while the lowest surfactant activity was determined for the cells grown at a salinity of 35 (0.9 pg T-X-100/L), as shown in Figure 5.

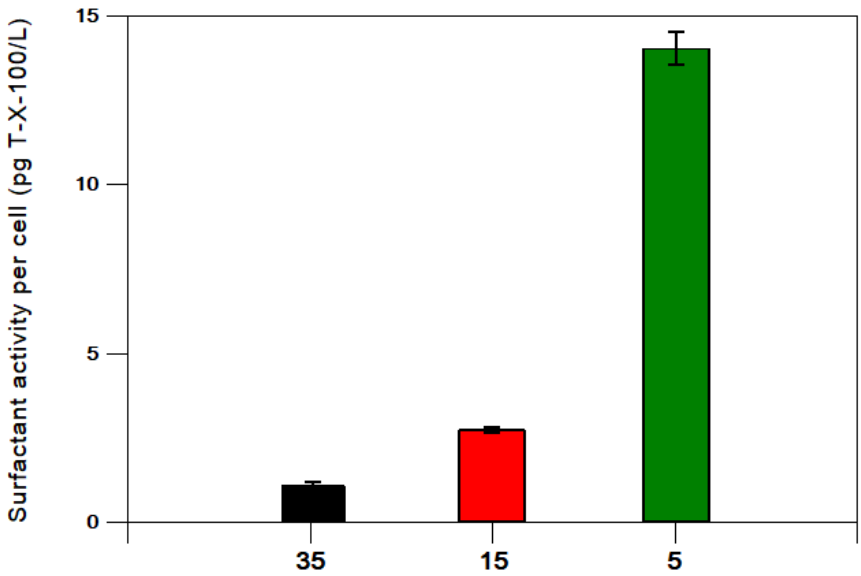

Figure 5. Surfactant activity of C. closterium cell cultures at selected salinities. *In each condition, the measurements were repeated with three different cultures.*

In addition, high-resolution AFM imaging was used to characterize the supramolecular organization of EPS at selected salinities, as presented in Figure 6). In each case, 10 diatoms were characterized. The results showed that at all salinities studied, the diatoms were surrounded by a dense layer (Figure 6a, d, g) that could extend up to 10 µm beyond the cell and was only a few nm thick. The difference in EPS organization as a function of salinity is very striking in these images. In cells grown at salinity of 35, only short individual fibrils can be seen (1-2 nm high, Figure 6 b and c), whereas in cells grown at salinities of 15 and 5, the EPS form a fibrillar network.

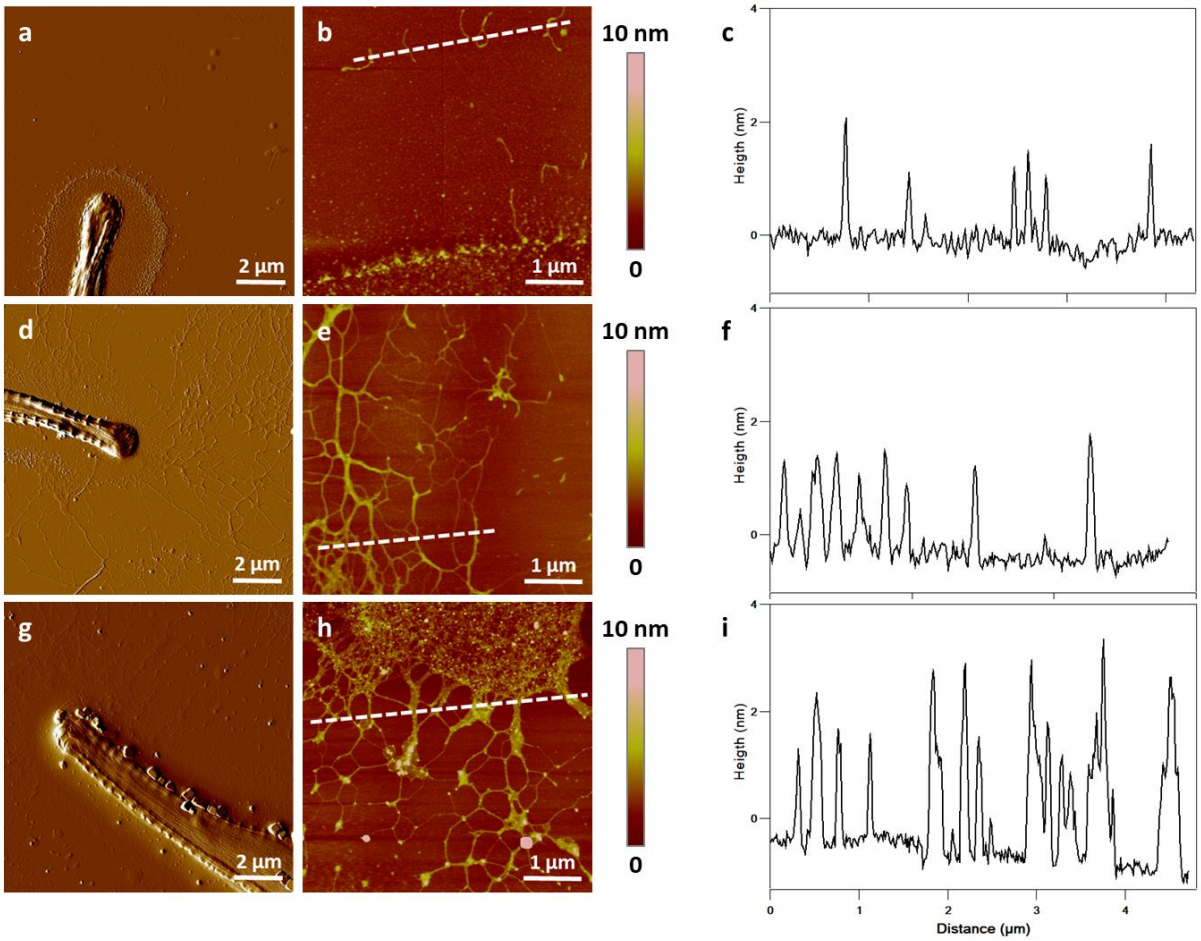

Figure 6. AFM characterization of the EPS produced by C. closterium cells at selected salinities. *AFM vertical deflection obtained in contact mode in air of C. closterium cell rostra at salinities of (a) 35, (d) 15 and (g) 5. (b), (e) and (h) are AFM height images recorded on closed-up 5 x 5 µm areas, respectively. (c), (f) and (i) are cross-sections taken along the white lines in (b), (e) and (h) respectively.*

4. DISCUSSION

Diatom aggregates that form in natural environments contribute significantly to marine snow. Their sedimentation has several effects, the most important being the export of organic material from the surface to the deep sea (Iversen and Ploug, 2013; Thornton, 2002). Because salinity is one of the most important fluctuating parameters in coastal and estuarine regions where *C. closterium* is common, it is important to evaluate the effects of hypo-saline conditions on cell aggregation. While the effects of hyper- or hypo-saline conditions on diatoms have been studied, the aggregation mechanism in diatoms during the exponential growth phase is poorly understood. In this study, we investigated the effects of hypo-saline conditions on the aggregation behaviour of *C. closterium* cells, and nanoscale characterization of cells and released EPS helped to elucidate the corresponding aggregation mechanism. To conduct this study, cells were characterized after 7 days of culture in hypo-saline conditions, where they are stressed and most likely not yet fully acclimated to the new saline regime, as acclimation takes place over longer time-scales (Borowitzka, 2018).

An initial aspect of the study was to determine the effects of hypo-saline conditions on cell growth dynamics. Several studies in the literature have examined the effects of altering salinity on *C. closterium* growth. Rijstenbil *et al.* found that high salinity had a significant negative effect on the photosynthetic activities of cells (Rijstenbil, 2005), whereas Van Bergeijk *et al*. reported that lower salinity levels (11 and 22 psu) had little effect on the growth rate of *C. closterium* cells or on the cell yield of long-term cultures (14 days) (Van Bergeijk et al., 2003). Our results are not consistent with these findings; however, in our case, the effects of reduced salinity on cells in the exponential growth phase were examined, which could explain the differences observed. In addition, it has been showed that different strains of *C. closterium* have distinct growth response patterns in terms of optimum growth temperature, which might also be the case for salinity (Stock et al., 2019). However, the results are consistent with our recent study that showed that favourable growth conditions for *C. closterium* are at salinities of 27 and 38 (Novosel et al., 2022a). Another study conducted with different strains of *C. closterium* isolated from brackish and marine habitats also found that reduced salinity stopped or slowed cell growth in 7-day cultures, confirming our findings (Glaser and Karsten, 2020). Finally, this effect of reduced salinity was also reported by Araujo and coworkers on 72-hour cultures of *C. closterium* (Araújo et al., 2013).

In a second step, the aggregation of cells under hypo-saline conditions was then quantified using flocculation/flotation experiments. The results showed a statistically significant decrease in cell aggregation under hypo-saline conditions. Because EPS has been reported to be an important factor promoting flocculation for several microalgal species (Steele et al., 2014; Vergnes et al., 2019), the experiments were additionally repeated with washed cells, where the majority of EPS was likely removed. The results highlight the important contribution of EPS to cell aggregation behaviour. However, even when most of the EPS was removed, the cells formed aggregates, but significantly less under hypo-saline conditions. This suggests that the EPS present in the culture medium are not the only factor affecting aggregation. To understand this, several hypotheses can be made: (i) salinity affects cell surface properties, (ii) salinity affects released EPS, and (iii) the combination of both factors, cell surface properties and released EPS, affects cell aggregation. To answer these questions, we examined the surface roughness and surface properties of *C. closterium* at the selected salinities. The surface of *C. closterium* in the exponential growth phase is very smooth, as revealed by roughness measurements in liquid, with an average roughness of 0.8 ± 0.2 nm. In a previous study, roughness measurements on *C. closterium* cells in the stationary growth phase gave roughness values in the range of 2 - 5 nm for salinities of 9, 19, 27, and 38 (Novosel et al., 2022a). Higher cell roughness values could be related to roughness measurements in air. In addition, cell roughness depends on the species and stressor. Some microalgal species had a smooth surface, such as *Chlorella vulgaris* (0.9 nm at pH 6, (Demir et al., 2020)), while the diatom *Phaeodactylum tricornutum* had a much rougher surface with values ranging from 5 to 10 nm (Ma et al., 2021). Finally, another study investigated the roughness of the diatom *Nitzschia closterium* under selected salinity conditions. Their results showed that the cell surface was rougher at a salinity of 18 (9.9 nm compared to 6.3 nm at a salinity of 32) due to the presence of silica particles on the cell surface, which is therefore not the case here (Ma et al., 2019).

As for the nanomechanical measurements performed, our results show that a decrease in salinity leads to an increase in cell rigidity. Several studies have shown that a change in environmental conditions can have an important impact on the composition or remodeling of the cell wall, changing its nanomechanical properties (Demir et al., 2020; Formosa-Dague et al., 2018;

Francius et al., 2008; Ma et al., 2019; Novosel et al., 2022a, 2022b). In particular, our previous study of *C. closterium* cells in stationary phase has shown that hypo-saline conditions leads to a marked increase in the production of membrane sterols, which make the cells significantly stiffer and more hydrophobic (Novosel et al., 2022a; Vrana et al., 2022). Perhaps a similar mechanism takes place here in the exponential phase. Moreover, changes in nanomechanical properties upon stress have also been reported in other microalgal species; for example, *P. tricornutum* and *C. vulgaris* cells exhibit increased stiffness at elevated pH (Demir et al., 2020; Formosa-Dague et al., 2018). In contrast, Ma and co-authors reported no effects on cell rigidity when *N. closterium* cells were exposed to hypo-saline conditions (Ma et al., 2019). However, in this case, Ym values obtained with a different model than that of this study were much higher (about 30 MPa), reflecting the higher content of silica in the cell wall of *N. closterium* compared to *C. closterium* and perhaps explaining the difference with our results.

Hydrophobicity of microalgal cells is also an important factor in aggregation efficiency (Garg et al., 2012; Ozkan and Berberoglu, 2013; Novosel et al., 2022a, 2022b). We investigated the hydrophobicity of *C. closterium* cells in the exponential growth phase at selected salinities. Results showed that diatoms grown under favorable conditions (salinity of 35) behaved more hydrophobically than cells grown under hypo-saline conditions, possibly promoting efficient aggregation compared to cells grown at lower salinities. These changes in cell hydrophobicity at different salinity variation suggest a chemical change in lipid metabolism (Novosel et al., 2022a; Vrana et al., 2022). In addition, cell surface properties have been shown to vary with cell age. For example, *D. tertiolecta* cells behave hydrophobic and stiff in exponential phase and under favorable growth conditions, while they are hydrophilic and soft in stationary phase, also suggesting a molecular change in their cell barrier (Pillet et al., 2019).

Regarding the release of EPS, an electrochemical approach allows quantification of the released surface-active organic matter, while AFM imaging provides insights into their nanostructural organisation. The results showed that the production of EPS was about 14 times higher in cells grown under hypo-saline conditions. Overproduction of EPS as a response of cells was reported when *C. closterium* was exposed to the heavy metal cadmium (Mišić Radić et al., 2021). Such behavior was also observed by Staats *et al.* who found that cultures of *C. closterium* depleted of nitrogen also produced more EPS (Staats et al., 2000). For example, under hyper-saline conditions, it has been shown for *P. tricornutum* cells that increased salinity increases the production of EPS with higher levels of uronic acids and sulphates, possibly allowing EPS to retain more water (Abdullahi et al., 2006). Thus, the higher amount of EPS at salinity 5 (as an unfavorable condition) corresponds to a response of cells to protect themselves against osmotic stress. Regarding the EPS nanostructure, the AFM results showed that the EPS are structured differently depending on the salinity: At salinity 35, the EPS form short single fibrils around the cells, while at salinity 15 and 5, the EPS form a fibrillar network. For *C. closterium* cells in stationary phase, our recent study showed a similar trend, with denser fibrils around the diatoms at lower salinities (9 and 19) with a higher degree of cross-linking (Novosel et al., 2022a). As the flocculation/flotation results showed, the EPS play an important role in flocculation, as for all conditions the separation efficiency and thus aggregation decreases by a factor of 3 when the EPS are removed from the cells. It is important to note that the cells aggregate independently of EPS production, implying that the EPS are not the only parameter that triggers cell aggregation at the selected salinities. As mentioned earlier, cell aggregation independent of the

presence of EPS also appears to be driven by the hydrophobic properties of the cells, which allow diatom aggregates to form at salinity 35.

5. CONCLUSIONS

We examined the effects of selected salinities that simulate changes from the euhaline to the mesohaline range to better understand how salinity changes impact diatom at the single cell level. Our results show that hypo-saline conditions reduce the ability of diatoms to form flocs during the exponential growth phase. To explain this behavior, we characterized both the surface properties of the cells and the EPS released. The AFM results show that the cells are significantly softer and more hydrophobic at a salinity of 35 than under hypo-saline conditions. The amount of EPS released and nanostructural organization were also found to be salinity dependent. At salinity of 35, diatoms released a small amount of EPS organized in short fibrils and still formed diatom aggregates. This can be explained by the fact that cells grown under favorable conditions are more hydrophobic than cells under hypo-saline stress, as hydrophobicity is an important factor promoting cell flocculation. This comprehensive study revealed the complex interplay between cell surface properties and physiological activity on the mechanism of diatom aggregation, which could lead to a fundamental understanding of their survival strategy under hypo-saline conditions in aquatic systems and also serve for biotechnological applications. Furthermore, because diatom aggregations in marine environments can have important impacts on ecosystems and the export of organic matter to the water column, these results provide fundamental data needed to understand these phenomena on a large scale.

Acknowledgements

C. F.-D. is a researcher at CNRS. The authors want to thank Emma Regourd for her technical support on flocculation/flotation experiments. In addition, the authors want to thank Dr. Etienne Dague for withdrawing the seawater used in part of this study during his scuba-diving trip with Ecole de Plongée Toulsaine (EPT) in Ile du Levant, France.

Funding

This work was supported by the Croatian-French program "Cogito" partner Hubert Curien (Campus France n°46656ZC), by the Agence Nationale de la Recherche, JCJC project FLOTALG (ANR-18-CE43-0001-01) and by the Croatian Science Foundation project "From algal cell surface properties to stress markers for aquatic ecosystems" (IP-2018-01-5840).

Author contributions

I. Demir-Yilmaz: Data acquisition, analysis, and interpretation, Writing- review and editing. **N. Novosel**: Data acquisition, analysis, and interpretation, Writing- review and editing. **M. Levak Zorinc**: Data acquisition, analysis, and interpretation, Writing- review and editing. **T. Mišić Radić**: Data acquisition, analysis, and interpretation, Writing- review and editing. **M. Souad Ftouhi**: Data acquisition, analysis, and interpretation, writing- review and editing. **P. Guiraud**: conception of the work, data interpretation, writing – review and editing. **N. Ivošević DeNardis**: Funding acquisition, conception of the work, data interpretation, writing – original draft. **C. Formosa-Dague**: Funding

acquisition, conception of the work, data acquisition, analysis and interpretation, writing – original draft.

Declarations

The authors have no competing interests to declare that are relevant to the content of this article.

Data availability statement

The datasets generated during and/or analyzed during the current study are available from the corresponding author on reasonable request.

References

Abdullahi, A.S., Underwood, G.J.C., Gretz, M.R., 2006. Extracellular Matrix Assembly in Diatoms (bacillariophyceae). V. Environmental Effects on Polysaccharide Synthesis in the Model Diatom, Phaeodactylum Tricornutum1. Journal of Phycology 42, 363–378. https://doi.org/10.1111/j.1529-8817.2006.00193.x

Alcoverro, T., Conte, E., Mazzella, L., 2000. Production of Mucilage by the Adriatic Epipelic Diatom Cylindrotheca Closterium (bacillariophyceae) Under Nutrient Limitation. Journal of Phycology 36, 1087–1095. https://doi.org/10.1046/j.1529-8817.2000.99193.x

Apoya-Horton, M.D., Yin, L., Underwood, G.J.C., Gretz, M.R., 2006. Movement Modalities and Responses to Environmental Changes of the Mudflat Diatom Cylindrotheca Closterium (bacillariophyceae)1. Journal of Phycology 42, 379–390. https://doi.org/10.1111/j.1529-8817.2006.00194.x

Araújo, C.V.M., Romero-Romero, S., Lourençato, L.F., Moreno-Garrido, I., Blasco, J., Gretz, M.R., Moreira-Santos, M., Ribeiro, R., 2013. Going with the Flow: Detection of Drift in Response to Hypo-Saline Stress by the Estuarine Benthic Diatom Cylindrotheca closterium. PLOS ONE 8, e81073. https://doi.org/10.1371/journal.pone.0081073

Besson, A., Formosa-Dague, C., Guiraud, P., 2019. Flocculation-flotation harvesting mechanism of Dunaliella salina: From nanoscale interpretation to industrial optimization. Water Research 155, 352–361. https://doi.org/10.1016/j.watres.2019.02.043

Besson, A., Guiraud, P., 2013. High-pH-induced flocculation-flotation of the hypersaline microalga Dunaliella salina. Bioresour. Technol. 147, 464–470. https://doi.org/10.1016/j.biortech.2013.08.053

Borowitzka, M.A., 2018. The 'stress' concept in microalgal biology—homeostasis, acclimation and adaptation. J Appl Phycol 30, 2815–2825. https://doi.org/10.1007/s10811-018-1399-0

Bussard, A., Corre, E., Hubas, C., Duvernois-Berthet, E., Le Corguillé, G., Jourdren, L., Coulpier, F., Claquin, P., Lopez, P.J., 2017. Physiological adjustments and transcriptome reprogramming are involved in the acclimation to salinity gradients in diatoms. Environmental Microbiology 19, 909–925. https://doi.org/10.1111/1462-2920.13398

de Brouwer, J.F.C., Wolfstein, K., Ruddy, G.K., Jones, T.E.R., Stal, L.J., 2005. Biogenic Stabilization of Intertidal Sediments: The Importance of Extracellular Polymeric Substances Produced by Benthic Diatoms. Microb Ecol 49, 501–512. https://doi.org/10.1007/s00248-004-0020-z

De Miranda, M., Gaviano, M., Serra, E., 2005. Changes in the cell size of the diatom Cylindrotheca closterium in a hyperhaline pond. Chemistry and Ecology 21, 77–81. https://doi.org/10.1080/02757540512331323962

Demir, I., Blockx, J., Dague, E., Guiraud, P., Thielemans, W., Muylaert, K., Formosa-Dague, C., 2020. Nanoscale Evidence Unravels Microalgae Flocculation Mechanism Induced by Chitosan. ACS Appl. Bio Mater. 3, 8446–8459. https://doi.org/10.1021/acsabm.0c00772

Demir, I., Lüchtefeld, I., Lemen, C., Dague, E., Guiraud, P., Zambelli, T., Formosa-Dague, C., 2021. Probing the interactions between air bubbles and (bio)interfaces at the nanoscale using FluidFM technology. Journal of Colloid and Interface Science 604, 785–797. https://doi.org/10.1016/j.jcis.2021.07.036

Demir-Yilmaz, I., Guiraud, P., Formosa-Dague, C., 2021. The contribution of Atomic Force Microscopy (AFM) in microalgae studies: A review. Algal Research 60, 102506. https://doi.org/10.1016/j.algal.2021.102506

Demir-Yilmaz, I., Yakovenko, N., Roux, C., Guiraud, P., Collin, F., Coudret, C., ter Halle, A., Formosa-Dague, C., 2022. The role of microplastics in microalgae cells aggregation: A study at the molecular scale using atomic force microscopy. Science of The Total Environment 832, 155036. https://doi.org/10.1016/j.scitotenv.2022.155036

Formosa-Dague, C., Gernigon, V., Castelain, M., Daboussi, F., Guiraud, P., 2018. Towards a better understanding of the flocculation/flotation mechanism of the marine microalgae Phaeodactylum tricornutum under increased pH using atomic force microscopy. Algal Research 33, 369–378. https://doi.org/10.1016/j.algal.2018.06.010

Francius, G., Tesson, B., Dague, E., Martin-Jézéquel, V., Dufrêne, Y.F., 2008. Nanostructure and nanomechanics of live Phaeodactylum tricornutum morphotypes. Environ. Microbiol. 10, 1344–1356. https://doi.org/10.1111/j.1462-2920.2007.01551.x

Garg, S., Li, Y., Wang, L., Schenk, P.M., 2012. Flotation of marine microalgae: effect of algal hydrophobicity. Bioresour. Technol. 121, 471–474. https://doi.org/10.1016/j.biortech.2012.06.111

Glaser, K., Karsten, U., 2020. Salinity tolerance in biogeographically different strains of the marine benthic diatom Cylindrotheca closterium (Bacillariophyceae). J Appl Phycol 32, 3809–3816. https://doi.org/10.1007/s10811-020-02238-6

Guillard, R.R.L., 1975. Culture of Phytoplankton for Feeding Marine Invertebrates, in: Smith, W.L., Chanley, M.H. (Eds.), Culture of Marine Invertebrate Animals: Proceedings — 1st Conference on Culture of Marine Invertebrate Animals Greenport. Springer US, Boston, MA, pp. 29–60. https://doi.org/10.1007/978-1-4615-8714-9_3

Hertz, H., 1881. Ueber die beruhrung fester elastischer korper. Journal fur die reine und angewandte mathematik 156–171.

Hutter, J.L., Bechhoefer, J., 1993. Calibration of atomic-force microscope tips. Review of Scientific Instruments 64, 1868–1873. https://doi.org/10.1063/1.1143970

Iversen, M.H., Ploug, H., 2013. Temperature effects on carbon-specific respiration rate and sinking velocity of diatom aggregates – potential implications for deep ocean export processes. Biogeosciences 10, 4073–4085. https://doi.org/10.5194/bg-10-4073-2013

Karsten, U., 2012. Seaweed Acclimation to Salinity and Desiccation Stress, in: Wiencke, C., Bischof, K. (Eds.), Seaweed Biology: Novel Insights into Ecophysiology, Ecology and Utilization, Ecological Studies. Springer, Berlin, Heidelberg, pp. 87–107. https://doi.org/10.1007/978-3-642-28451-9_5

Kim, S.-K., 2015. Handbook of Marine Microalgae: Biotechnology Advances, Academic Press. ed. London.

Kovač, N., Mozetič, P., Trichet, J., Défarge, C., 2005. Phytoplankton composition and organic matter organization of mucous aggregates by means of light and cryo-scanning electron microscopy. Marine Biology 147, 261–271. https://doi.org/10.1007/s00227-004-1531-3

Ma, J., Zhou, B., Chen, F., Pan, K., 2021. How marine diatoms cope with metal challenge: Insights from the morphotype-dependent metal tolerance in Phaeodactylum tricornutum. Ecotoxicology and Environmental Safety 208, 111715. https://doi.org/10.1016/j.ecoenv.2020.111715

Ma, J., Zhou, B., Duan, D., Pan, K., 2019. Salinity-dependent nanostructures and composition of cell surface and its relation to Cd toxicity in an estuarine diatom. Chemosphere 215, 807–814. https://doi.org/10.1016/j.chemosphere.2018.10.128

Meister, A., Gabi, M., Behr, P., Studer, P., Vörös, J., Niedermann, P., Bitterli, J., Polesel-Maris, J., Liley, M., Heinzelmann, H., Zambelli, T., 2009. FluidFM: combining atomic force microscopy and nanofluidics in a universal liquid delivery system for single cell applications and beyond. Nano Lett. 9, 2501–2507. https://doi.org/10.1021/nl901384x

Mišić Radić, T., Čačković, A., Penezić, A., Dautović, J., Lončar, J., Omanović, D., Juraić, K., Ljubešić, Z., 2021. Physiological and morphological response of marine diatom Cylindrotheca closterium (Bacillariophyceae) exposed to Cadmium. European Journal of Phycology 56, 24–36. https://doi.org/10.1080/09670262.2020.1758347

Najdek, M., Blažina, M., Djakovac, T., Kraus, R., 2005. The role of the diatom Cylindrotheca closterium in a mucilage event in the northern Adriatic Sea: coupling with high salinity water intrusions. Journal of Plankton Research 27, 851–862. https://doi.org/10.1093/plankt/fbi057

Novosel, N., Mišić Radić, T., Levak Zorinc, M., Zemla, J., Lekka, M., Vrana, I., Gašparović, B., Horvat, L., Kasum, D., Legović, T., Žutinić, P., Gligora Udovič, M., Ivošević DeNardis, N., 2022a. Salinity-induced chemical, mechanical, and behavioral changes in marine microalgae. J Appl Phycol 34, 1293–1309. https://doi.org/10.1007/s10811-022-02734-x

Novosel, N., Mišić Radić, T., Zemla, J., Lekka, M., Čačković, A., Kasum, D., Legović, T., Žutinić, P., Gligora Udovič, M., Ivošević DeNardis, N., 2022b. Temperature-induced response in algal cell surface properties and behaviour: an experimental approach. J Appl Phycol 34, 243–259. https://doi.org/10.1007/s10811-021-02591-0

Ozkan, A., Berberoglu, H., 2013. Physico-chemical surface properties of microalgae. Colloids and Surfaces B: Biointerfaces 112, 287–293. https://doi.org/10.1016/j.colsurfb.2013.08.001

Pillet, F., Dague, E., Pečar Ilić, J., Ružić, I., Rols, M.-P., Ivošević DeNardis, N., 2019. Changes in nanomechanical properties and adhesion dynamics of algal cells during their growth. Bioelectrochemistry 127, 154–162. https://doi.org/voelcker

Piontek, J., Händel, N., Langer, G., Wohlers, J., Riebesell, U., Engel, A., 2009. Effects of rising temperature on the formation and microbial degradation of marine diatom aggregates. Aquatic Microbial Ecology 54, 305–318. https://doi.org/10.3354/ame01273

Pletikapić, G., Ivošević DeNardis, N., 2017. Application of surface analytical methods for hazardous situation in the Adriatic Sea: monitoring of organic matter dynamics and oil pollution. Natural Hazards and Earth System Sciences 17, 31–44. https://doi.org/10.5194/nhess-17-31-2017

Pletikapić, G., Radić, T.M., Zimmermann, A.H., Svetličić, V., Pfannkuchen, M., Marić, D., Godrijan, J., Žutić, V., 2011. AFM imaging of extracellular polymer release by marine diatom Cylindrotheca closterium (Ehrenberg) Reiman & J.C. Lewin. Journal of Molecular Recognition 24, 436–445. https://doi.org/10.1002/jmr.1114

Radić, T.M., Svetličić, V., Žutić, V., Boulgaropoulos, B., 2011. Seawater at the nanoscale: marine gel imaged by atomic force microscopy. Journal of Molecular Recognition 24, 397–405. https://doi.org/10.1002/jmr.1072

Rijstenbil, J.W., 2005. UV- and salinity-induced oxidative effects in the marine diatom Cylindrotheca closterium during simulated emersion. Marine Biology 147, 1063–1073. https://doi.org/10.1007/s00227-005-0015-4

Roncarati, F., Rijstenbil, J.W., Pistocchi, R., 2008. Photosynthetic performance, oxidative damage and antioxidants in Cylindrotheca closterium in response to high irradiance, UVB radiation and salinity. Mar Biol 153, 965–973. https://doi.org/10.1007/s00227-007-0868-9

Scala, S., Bowler, C., 2001. Molecular insights into the novel aspects of diatom biology. Cell. Mol. Life Sci. 58, 1666–1673. https://doi.org/10.1007/PL00000804

Staats, N., Stal, L.J., Mur, L.R., 2000. Exopolysaccharide production by the epipelic diatom Cylindrotheca closterium: effects of nutrient conditions. Journal of Experimental Marine Biology and Ecology 249, 13–27. https://doi.org/10.1016/S0022-0981(00)00166-0

Steele, D.J., Franklin, D.J., Underwood, G.J.C., 2014. Protection of cells from salinity stress by extracellular polymeric substances in diatom biofilms. Biofouling 30, 987–998. https://doi.org/10.1080/08927014.2014.960859

Stock, W., Vanelslander, B., Rüdiger, F., Sabbe, K., Vyverman, W., Karsten, U., 2019. Thermal Niche Differentiation in the Benthic Diatom Cylindrotheca closterium (Bacillariophyceae) Complex. Frontiers in Microbiology 10.

Svetličić, V., Balnois, E., Žutić, V., Chevalet, J., Hozić Zimmermann, A., Kovač, S., Vdović, N., 2006. Electrochemical Detection of Gel Microparticles in Seawater. Croatica Chemica Acta 79, 107–113.

Svetličić, V., Žutić, V., Radić, T.M., Pletikapić, G., Zimmermann, A.H., Urbani, R., 2011. Polymer Networks Produced by Marine Diatoms in the Northern Adriatic Sea. Marine Drugs 9, 666–679. https://doi.org/10.3390/md9040666

Thornton, D.C.O., 2002. Diatom aggregation in the sea: mechanisms and ecological implications. European Journal of Phycology 37, 149–161. https://doi.org/10.1017/S0967026202003657

Tréguer, P., Bowler, C., Moriceau, B., Dutkiewicz, S., Gehlen, M., Aumont, O., Bittner, L., Dugdale, R., Finkel, Z., Iudicone, D., Jahn, O., Guidi, L., Lasbleiz, M., Leblanc, K., Levy, M., Pondaven, P., 2018. Influence of diatom diversity on the ocean biological carbon pump. Nature Geosci 11, 27–37. https://doi.org/10.1038/s41561-017-0028-x

Van Bergeijk, S.A., Van der Zee, C., Stal, L.J., 2003. Uptake and excretion of dimethylsulphoniopropionate is driven by salinity changes in the marine benthic diatom Cylindrotheca closterium. European Journal of Phycology 38, 341–349. https://doi.org/10.1080/0967026031000161260O

Vergnes, J.B., Gernigon, V., Guiraud, P., Formosa-Dague, C., 2019. Bicarbonate Concentration Induces Production of Exopolysaccharides by Arthrospira platensis That Mediate Bioflocculation and Enhance Flotation Harvesting Efficiency. ACS Sustainable Chem. Eng. 7, 13796–13804. https://doi.org/10.1021/acssuschemeng.9b01591

Vrana, I., Bakija Alempijević, S., Novosel, N., Ivošević DeNardis, N., Žigon, D., Ogrinc, N., Gašparović, B., 2022. Hyposalinity induces significant polar lipid remodeling in the marine microalga Dunaliella tertiolecta (Chlorophyceae). J Appl Phycol 34, 1457–1470. https://doi.org/10.1007/s10811-022-02745-8

Žutić, V., Svetličić, S., 2000. Interfactial processes, in: Wangersky, P. (Ed.), The Handbook of Environmental Chemistry1. Springer Verlag, Berlin, Germany, pp. 149–165.